Supplementary Information (SI) for Journal of Materials Chemistry A.

Supplementary material

Aqueous synthesis of lithium superionic−conducting complex hydride solid electrolytes

Hyerim Kim[a], Taehyun Kim[a], Seunghee Joo[a], Jeonghyun Kim[a], Jaehyun Noh[a,b], Jiyoung Ma[b] Jung−Je Woo[b], Seungho Choi[c], Kyungsu Kim[c], Woosuk Cho[c], Kazuaki Kisu[d], Shin−ichi Orimo[d,e], and Sangryun Kim[a,*]

[a]*Graduate School of Energy Convergence, Gwangju Institute of Science and Technology (GIST), 123 Cheomdangwagi−ro, Gwangju 61005, Republic of Korea*

[b]*Gwangju Clean Energy Research Center, Korea Institute of Energy Research (KIER), 270−25 Samso−ro, Gwangju 61003, Republic of Korea*

[c]*Advanced Batteries Research Center, Korea Electronics Technology Institute, 25 Saenari−ro, Seongnam 13509, Republic of Korea*

[d]*Institute for Materials Research (IMR), Tohoku University, Katahira 2−1−1, Sendai 980−8577, Japan*

[e]*WPI−Advanced Institute for Materials Research (WPI−AIMR), Tohoku University, Katahira 2−1−1, Sendai 980−8577, Japan*

[*]Corresponding author

E-mail address: sangryun@gist.ac.kr

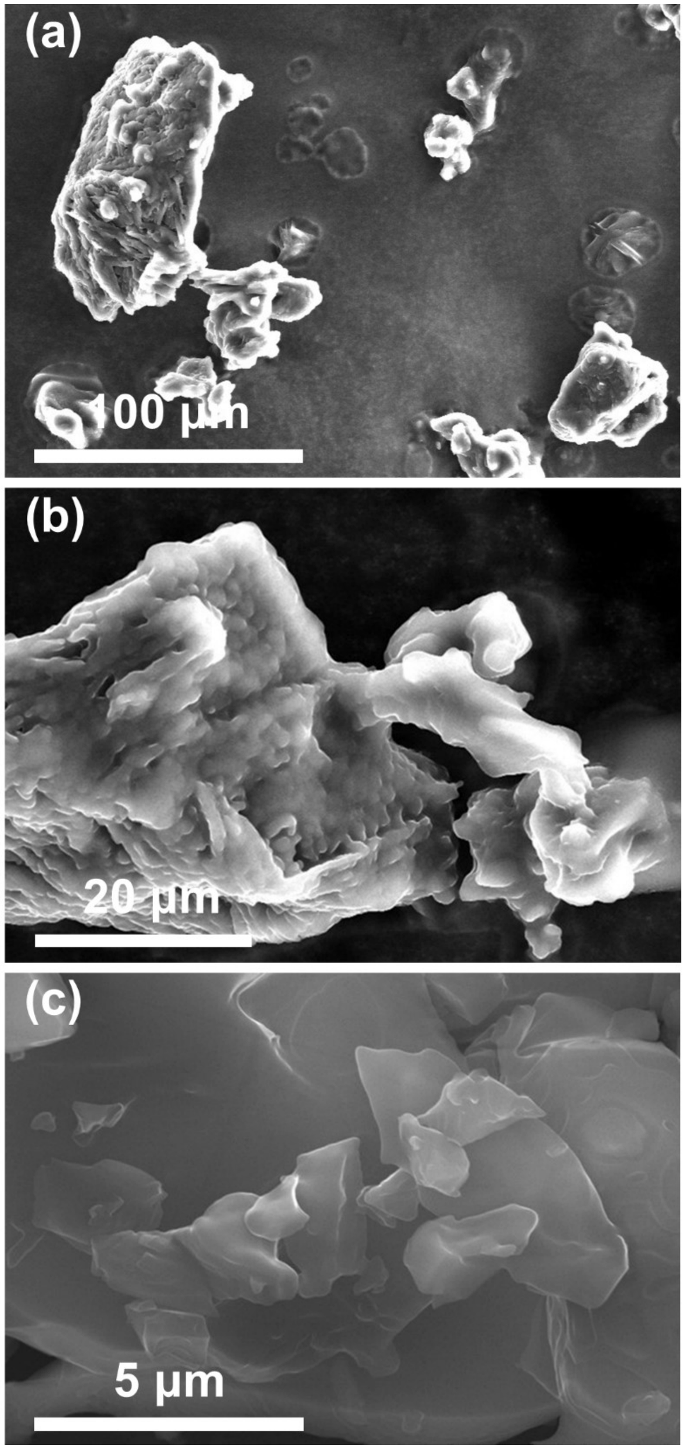

Fig. S1. FE−SEM images of $Li(CB_9H_{10})_{0.7}(CB_{11}H_{12})_{0.3}$ prepared by the liquid–phase synthesis: (a) Scale bar, 100 µm, (b) Scale bar, 20 µm, and (c) Scale bar, 5 µm.

Table S1. Ionic conductivities and activation energies of $Li(CB_9H_{10})_{0.7}(CB_{11}H_{12})_{0.3}$ prepared by solid−phase and liquid−phase synthesis.

Material	Synthetic method	Ionic conductivity (S cm^{-1})	Activation energy (kJ mol^{-1})	References
$Li(CB_9H_{10})_{0.7}(CB_{11}H_{12})_{0.3}$	Solid−phase	6.7×10^{-3} (25 °C) 8.5×10^{-2} (110 °C)	28.4	1
	Liquid−phase	6.6×10^{-3} (25 °C) 9.5×10^{-2} (110 °C)	29.2	Present study

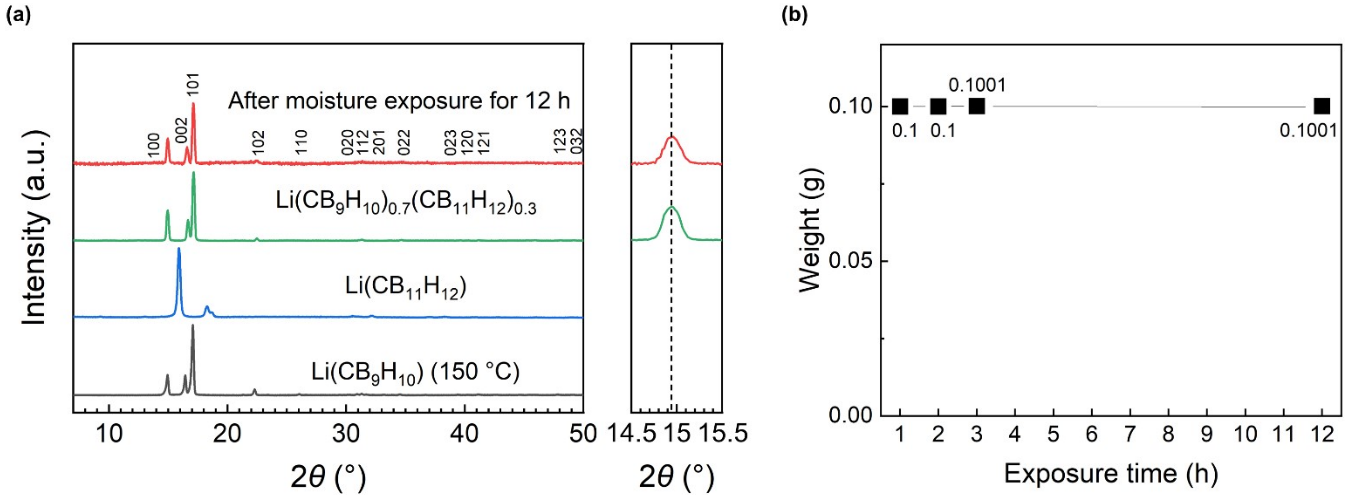

Fig. S2. (a) XRD patterns of $Li(CB_9H_{10})$, $Li(CB_{11}H_{12})$, and $Li(CB_9H_{10})_{0.7}(CB_{11}H_{12})_{0.3}$ before and after moisture exposure at a dew point of −50 °C for 12 h. (b) Change in the weight of the $Li(CB_9H_{10})_{0.7}(CB_{11}H_{12})_{0.3}$ powder during moisture exposure at a dew point of −50 °C.

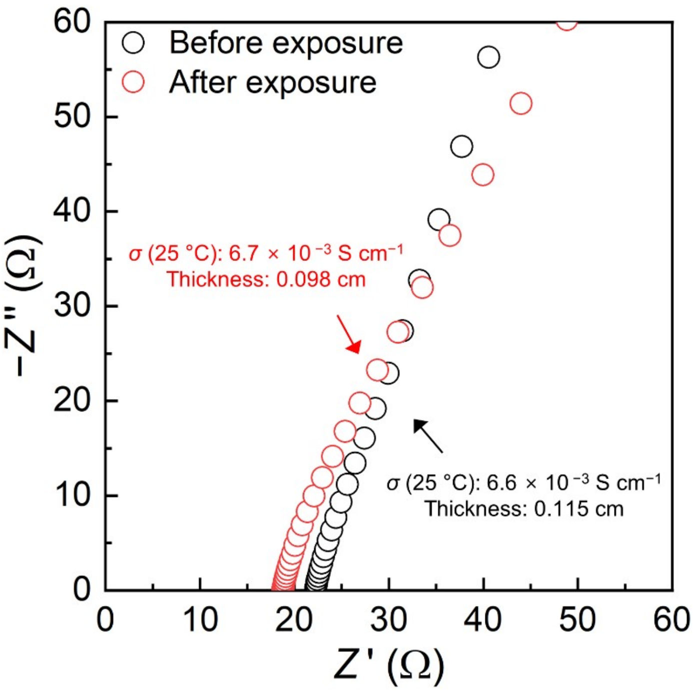

Fig. S3. Nyquist plots of $Li(CB_9H_{10})_{0.7}(CB_{11}H_{12})_{0.3}$ at 25 °C before and after moisture exposure at a dew point of −50 °C for 12 h.

Table S2. Used solvents, synthetic temperatures, and ionic conductivities of various solid electrolytes synthesized by the liquid−phase method.

Material	Solvent	Synthetic temperature[a] (°C)	Ionic conductivity[b] (S cm^{-1})	References
$Li(CB_9H_{10})_{0.7}(CB_{11}H_{12})_{0.3}$	DI water	200	6.6×10^{-3}	This work
$Li_7P_2S_8I$	ACN[c]	200	6.3×10^{-4}	2
$Li_7P_2S_8I$	EP[d]	170	4.7×10^{-4}	3
$Li_7P_3S_{11}$	ACN	180	1.0×10^{-3}	4
$Li_7P_3S_{11}$	THF[e]−ACN	250	9.7×10^{-4}	5
$Li_7P_3S_{11}$	ACN	260	1.5×10^{-3}	6
$Li_7P_3S_{11}$	DME[f]	250	2.7×10^{-4}	7
Li_6PS_5Cl	Ethanol−THF	550	2.2×10^{-3}	8
Li_6PS_5Cl	ACN−PTH[g]	550	2.8×10^{-3}	9
Li_6PS_5Cl	EA[h]	550	1.1×10^{-3}	10
Li_6PS_5Cl	Ethanol	80	1.4×10^{-5}	11
Li_6PS_5Cl	Ethanol−ACN	180	6×10^{-4}	12
Li_6PS_5Cl	THF−Ethanol	550	2.4×10^{-3}	13
Li_6PS_5Cl	THF	550	2.2×10^{-3}	14
Li_6PS_5Cl	Anisole−Ethanol	550	2.1×10^{-3}	15
$Li_{10}GeP_2S_{12}$	ACN−THF−Ethanol	550	1.6×10^{-3}	16
Li_7PS_6	Ethanol	200	1.1×10^{-4}	17
Li_6PS_5Br	THF−Ethanol	550	1.4×10^{-3}	18
Li_6PS_5Br	EP−Ethanol	180	3.4×10^{-5}	19
Li_6PS_5Br	Ethanol	150	1.9×10^{-4}	20
β−Li_3PS_4	THF	140	1.6×10^{-4}	21
β−Li_3PS_4	EA	160	3.3×10^{-4}	22
β−Li_3PS_4	ACN	200	1.2×10^{-4}	23
β−Li_3PS_4	THF	140	1.3×10^{-4}	24
Li_4PS_4I	DME	200	1.2×10^{-4}	25
Li_3PS_4−$LiBH_4$	THF	160	6.0×10^{-3}	26
$Li_{6.5}P_{0.5}GE_{0.5}S_5I$	Ethanol	180	5.4×10^{-4}	27

$Li_2S{-}P_2S_5$	Dibutyl ether	165	3.1×10^{-4}	28
Li_3InCl_6	DI water[i]	200	2.0×10^{-3}	29
$Li_{3.2}P_{0.8}Sn_{0.2}S_4$	EDA[j]−EDT[k]−THF	260	1.9×10^{-4}	30
Li_4SnS_4	DI water	320	1.4×10^{-4}	31
$0.6Li_4SnS_4{-}0.4LiI$	Methanol	200	4.1×10^{-4}	32
$Li_{6.28}Al_{0.24}La_3Zr_2O_{12}$	DI water	1200	5.1×10^{-4}	33
$Li_7La_3Zr_{1.89}Al_{0.15}O_{12}$	Nitric acid	1150	3.4×10^{-4}	34
$Li_{1.4}Al_{0.4}Ge_{1.6}(PO_4)_3$	Ethylene glycol	900	1.2×10^{-3}	35

[a]The highest heat treatment temperature in the previous reports; [b]Room temperature (22−30 °C) conductivity of the cold−pressed samples; [c]ACN, acetonitrile; [d]EP, ethyl propionate; [e]THF, tetrahydrofuran; [f]DME, 1,2−dimethoxyethane; [g]PTH, 1−propanethiol; [h]EA, ethyl acetate; [i]DI water, deionized water; [j]EDA, 1,2−ethylenediamine; [k]EDT, 1,2−ethanedithiol.

Table S3. Ionic conductivities of various solid electrolytes synthesized by the solid−phase and liquid−phase methods.

Material	Ionic conductivity[a] (S cm^{-1})		$\lvert 1 - \sigma_{Liquid-phase}/\sigma_{Solid-phase} \rvert$	References	
	Solid−phase synthesis	Liquid−phase synthesis		Solid−phase synthesis[b]	Liquid−phase synthesis
$Li(CB_9H_{10})_{0.7}(CB_{11}H_{12})_{0.3}$	6.7×10^{-3}	6.6×10^{-3}	0.01	1	This work
$Li_7P_3S_{11}$	3.2×10^{-3}	1.0×10^{-3}	0.69	36	4
$Li_7P_3S_{11}$	1.7×10^{-2}	9.7×10^{-4}	0.94	37	5
$Li_7P_3S_{11}$	2.9×10^{-3}	2.7×10^{-4}	0.91	38	7
Li_6PS_5Cl	2.1×10^{-3}	2.2×10^{-3}	0.04	8	8
Li_6PS_5Cl	2.9×10^{-3}	2.8×10^{-3}	0.05	9	9
Li_6PS_5Cl	2.9×10^{-3}	1.1×10^{-4}	0.62	10	10
Li_6PS_5Cl	1.4×10^{-3}	1.4×10^{-5}	0.99	11	11
Li_6PS_5Cl	3.0×10^{-3}	2.4×10^{-3}	0.85	39	13
Li_6PS_5Cl	4×10^{-5}	6×10^{-4}	14	12	12
$Li_{10}GeP_2S_{12}$	1.2×10^{-2}	1.6×10^{-3}	0.87	40	16
Li_6PS_5Br	1.9×10^{-3}	1.4×10^{-3}	0.26	18	18
Li_6PS_5Br	1.0×10^{-4}	3.4×10^{-5}	0.66	19	19
Li_6PS_5Br	8.2×10^{-4}	1.9×10^{-4}	0.77	20	20
$Li_2S-P_2S_5$	6.7×10^{-4}	3.1×10^{-4}	0.54	28	28
Li_3InCl_6	1.5×10^{-3}	2.0×10^{-3}	0.36	41	29
$Li_{3.2}P_{0.8}Sn_{0.2}S_4$	7.7×10^{-4}	1.9×10^{-4}	0.75	30	30
$\beta-Li_3PS_4$	8.9×10^{-7}	1.6×10^{-3}	1796.75	21	21
$\beta-Li_3PS_4$	4×10^{-6}	3.4×10^{-4}	84	42	22
$Li_{1.4}Al_{0.4}Ge_{1.6}(PO_4)_3$	3.5×10^{-6}	1.2×10^{-3}	347.57	43	35

[a]Room temperature (22−30 °C) conductivity of the cold−pressed samples. [b]Conductivity compared in the literature on the liquid−phase synthesis.

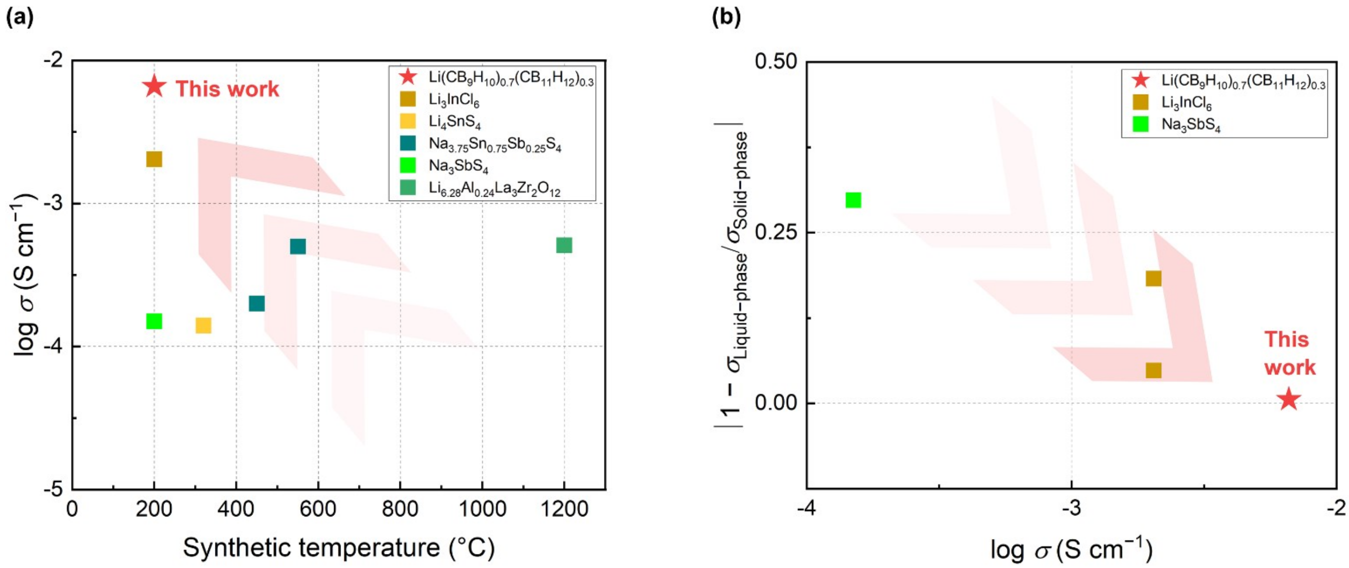

Fig. S4. (a) Ionic conductivities of various solid electrolytes synthesized by the aqueous liquid–phase method. (b) Change rates of ionic conductivities of the aqueous liquid−phase and solid−phase samples.

Table S4. Synthetic temperatures and ionic conductivities of various solid electrolytes synthesized by aqueous liquid–phase method.

Material	Solvent	Synthetic temperature[a] (°C)	Ionic conductivity[b] (S cm^{-1})	References
$Li(CB_9H_{10})_{0.7}(CB_{11}H_{12})_{0.3}$	DI water	200	6.6×10^{-3}	This work
Li_3InCl_6	DI water	200	2.0×10^{-3}	29
Li_4SnS_4	DI water	320	1.4×10^{-4}	31
$Na_{3.75}Sn_{0.75}Sb_{0.25}S_4$	DI water	450	2.0×10^{-4}	44
$Na_{3.75}Sn_{0.75}Sb_{0.25}S_4$	DI water	550	5.0×10^{-4}	44
Na_3SbS_4	DI water	200	1.5×10^{-4}	45
$Li_{6.28}Al_{0.24}La_3Zr_2O_{12}$	DI water	1200	5.1×10^{-4}	33

[a]The highest heat treatment temperature in the previous reports; [b]Room temperature (22−30 °C) conductivity of the cold−pressed samples.

Table S5. Ionic conductivities of various solid electrolytes synthesized by solid−phase and aqueous liquid−phase methods.

Material	Ionic conductivity[a] (S cm^{-1})		$\lvert 1 - \sigma_{\text{Liquid−phase}}/\sigma_{\text{Solid−phase}} \rvert$	References	
	Solid−phase synthesis	Liquid−phase synthesis		Solid−phase synthesis[b]	Liquid−phase synthesis
$Li(CB_9H_{10})_{0.7}(CB_{11}H_{12})_{0.3}$	6.7×10^{-3}	6.6×10^{-3}	0.01	1	This work
Li_3InCl_6	5.1×10^{-4}	2.0×10^{-3}	3	46	29
Li_3InCl_6	1.5×10^{-3}	2.0×10^{-3}	0.36	41	29
Na_3SbS_4	1.1×10^{-3}	1.5×10^{-4}	0.87	45	45
$Li_{1.4}Al_{0.4}Ge_{1.6}(PO_4)_3$	3.5×10^{-6}	1.2×10^{-3}	347.57	43	35

[a]Room temperature (22−30 °C) conductivity of the cold−pressed samples. [b]Conductivity compared in the literature on the liquid−phase synthesis

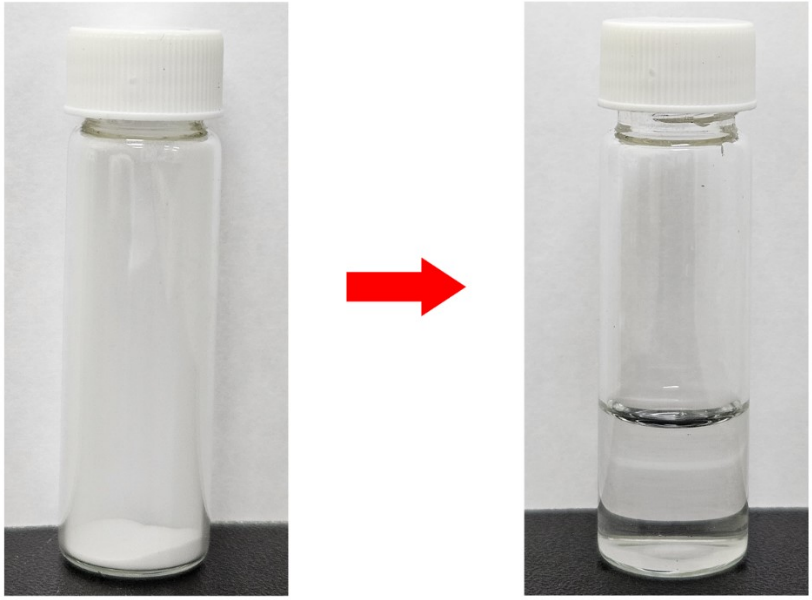

Fig. S5. Optical images before and after the dissolution of the $Li(CB_9H_{10})$ powder in DI water.

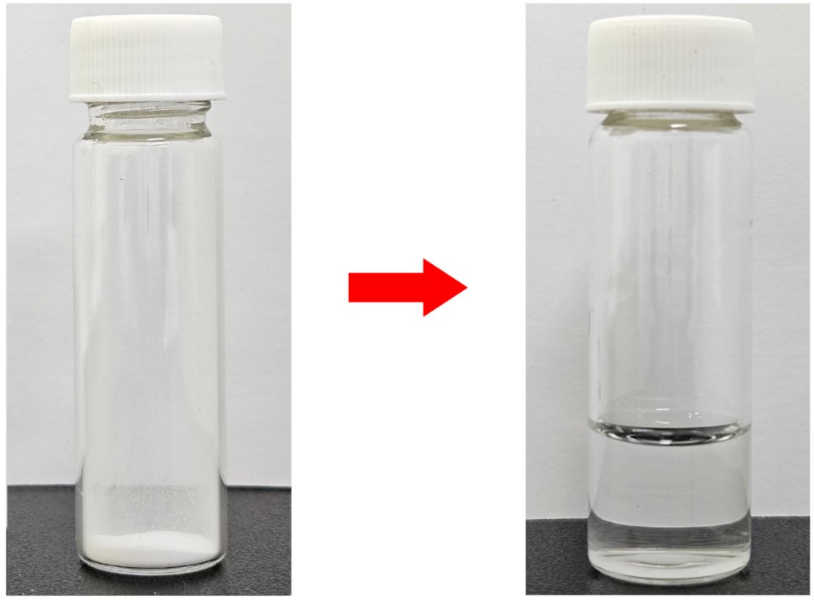

Fig. S6. Optical images before and after the dissolution of the $Li(CB_{11}H_{12})$ powder in DI water.

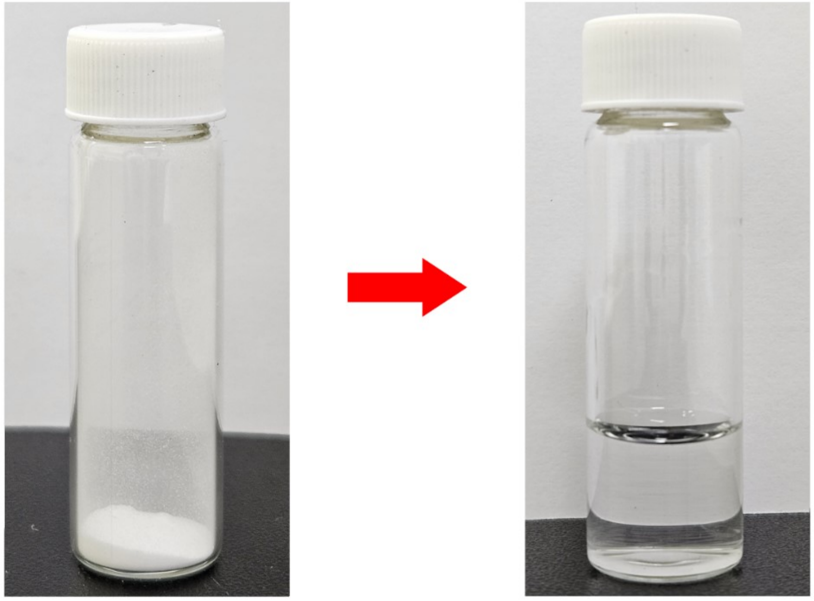

Fig. S7. Optical images before and after the dissolution of the $Li(CB_9H_{110})$ and $Li(CB_{11}H_{12})$ powders in DI water.

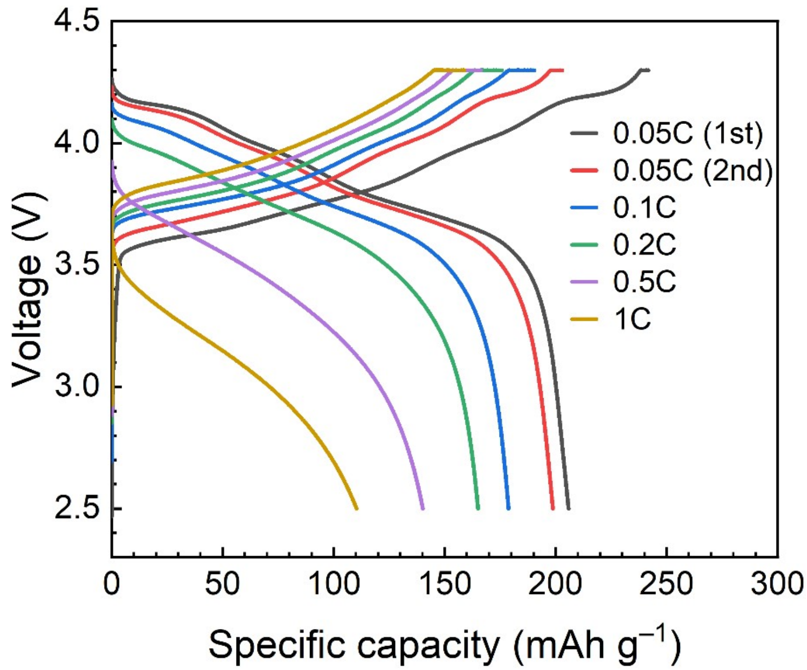

Fig. S8. Charge−discharge profiles of the cell using Li_6PS_5Cl solid electrolyte at 0.05, 0.1, 0.2, 0.5, and 1C; at 0.1, 0.2, 0.5, and 1C, the charging rate is fixed as 0.1C. After the first cycle, as the C−rate increased by 2, 4, 10, and 20 times from 0.05C, the cell retained 89.9%, 85.6%, 70.5%, and 55.5% of the capacity (198.7 mAh g^{-1}) in the second cycle, respectively.

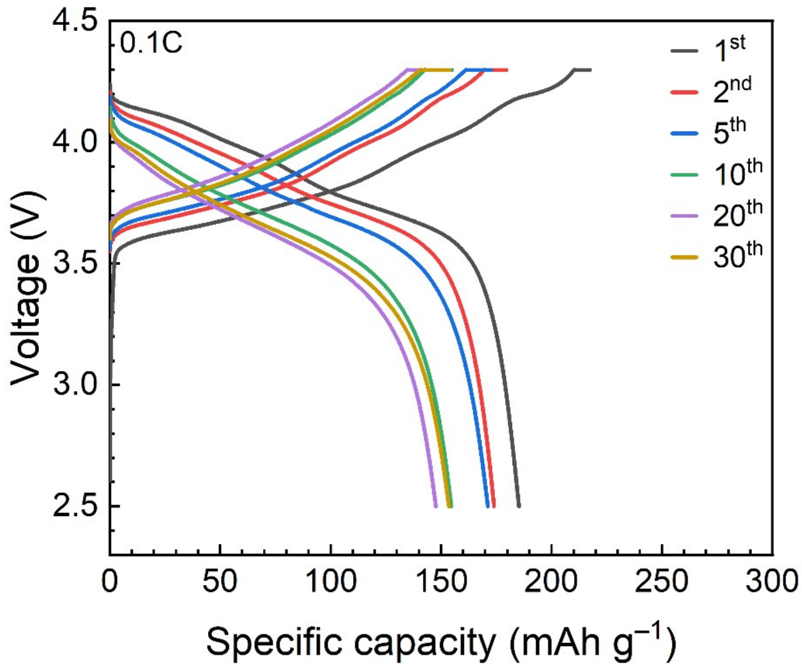

Fig. S9. Charge−discharge profiles of the cell using $Li(CB_9H_{10})_{0.7}(CB_{11}H_{12})_{0.3}$ solid electrolyte at 0.1 C and 40 °C.

REFERENCES

1. S. Kim, H. Oguchi, N. Toyama, T. Sato, S. Takagi, T. Otomo, D. Arunkumar, N. Kuwata, J. Kawamura and S.-I. Orimo, *Nat. Commun.*, 2019, **10**, 1081.
2. E. Rangasamy, Z. Liu, M. Gobet, K. Pilar, G. Sahu, W. Zhou, H. Wu, S. Greenbaum and C. Liang, *J. Am. Chem. Soc.*, 2015, **137**, 1384–1387.
3. N. H. H. Phuc, E. Hirahara, K. Morikawa, H. Muto and A. Matsuda, *J. Power Sources*, 2017, **365**, 7–11.
4. M. Calpa, N. C. Rosero-Navarro, A. Miura and K. Tadanaga, *Inorg. Chem. Front.*, 2018, **5**, 501–508.
5. R. C. Xu, X. H. Xia, Z. J. Yao, X. L. Wang, C. D. Gu and J. P. Tu, *Electrochim. Acta*, 2016, **219**, 235–240.
6. X. Yao, D. Liu, C. Wang, P. Long, G. Peng, Y.-S. Hu, H. Li, L. Chen and X. Xu, *Nano. Lett.*, 2016, **16**, 7148–7154.
7. S. Ito, M. Nakakita, Y. Aihara, T. Uehara and N. Machida, *J. Power Sources*, 2014, **271**, 342–345.
8. A. Han, R. Tian, L. Fang, F. Wan, X. Hu, Z. Zhao, F. Tu, D. Song, X. Zhang and Y. Yang, *ACS Appl. Mater. Interfaces*, 2022, **14**, 30824–30838.
9. R. F. Indrawan, H. Gamo, A. Nagai and A. Matsuda, *Chem. Mater.*, 2023, **35**, 2549–2558.
10. S. Choi, J. Ann, J. Do, S. Lim, C. Park and D. Shin, *J. Electrochem. Soc.*, 2019, **166**, A5193–A5200.
11. S. Yubuchi, S. Teragawa, K. Aso, K. Tadanaga, A. Hayashi and M. Tatsumisago, *J. Power Sources*, 2015, **293**, 941–945.
12. N. C. Rosero-Navarro, A. Miura and K. Tadanaga, *J. Power Sources*, 2018, **396**, 33–40.
13. L. Zhou, K.-H. Park, X. Sun, F. Lalère, T. Adermann, P. Hartmann and L. F. Nazar, *ACS Energy*

Lett., 2018, **4**, 265–270.

14. I.-H. Choi, E. Kim, Y.-S. Jo, J.-W. Hong, J. Sung, J. Seo, B. Kim, J.-h. Park, Y.-J. Lee, Y.-C. Ha, D. Kim, J. H. Lee and J.-W. Park, *J. Ind. Eng. Chem.*, 2023, **121**, 107–113.
15. R. Maniwa, M. Calpa, N. C. Rosero-Navarro, A. Miura and K. Tadanaga, *J. Mater. Chem. A*, 2021, **9**, 400–405.
16. K. Hikima, K. Ogawa, H. Gamo and A. Matsuda, *Chem. Commun.*, 2023, **59**, 6564–6567.
17. D. A. Ziolkowska, W. Arnold, T. Druffel, M. Sunkara and H. Wang, *ACS Appl. Mater. Interfaces*, 2019, **11**, 6015–6021.
18. S. Yubuchi, M. Uematsu, C. Hotehama, A. Sakuda, A. Hayashi and M. Tatsumisago, *J. Mater. Chem. A*, 2019, **7**, 558–566.
19. S. Chida, A. Miura, N. C. Rosero-Navarro, M. Higuchi, N. H. H. Phuc, H. Muto, A. Matsuda and K. Tadanaga, *Ceram. Int.*, 2018, **44**, 742–746.
20. S. Yubuchi, M. Uematsu, M. Deguchi, A. Hayashi and M. Tatsumisago, *ACS Appl. Energy Mater.*, 2018, **1**, 3622–3629.
21. Z. Liu, W. Fu, E. A. Payzant, X. Yu, Z. Wu, N. J. Dudney, J. Kiggans, K. Hong, A. J. Rondinone and C. Liang, *J. Am. Chem. Soc.*, 2013, **135**, 975–978.
22. N. H. H. Phuc, M. Totani, K. Morikawa, H. Muto and A. Matsuda, *Solid State Ion.*, 2016, **288**, 240–243.
23. H. Wang, Z. D. Hood, Y. Xia and C. Liang, *J. Mater. Chem. A*, 2016, **4**, 8091–8096.
24. H.-D. Lim, X. Yue, X. Xing, V. Petrova, M. Gonzalez, H. Liu and P. Liu, *J. Mater. Chem. A*, 2018, **6**, 7370–7374.
25. S. J. Sedlmaier, S. Indris, C. Dietrich, M. Yavuz, C. Dräger, F. von Seggern, H. Sommer and J. r. Janek, *Chem. Mater.*, 2017, **29**, 1830–1835.

26. D. Wang, L.-J. Jhang, R. Kou, M. Liao, S. Zheng, H. Jiang, P. Shi, G.-X. Li, K. Meng and D. Wang, *Nat. Commun.*, 2023, **14**, 1895.

27. Y. Song, D. Kim, H. Kwak, D. Han, S. Kang, J. Lee, S.-m. Bak, K. Nam, L. Hyun-wook and Y. Jung, *Nano. Lett.*, 2020, **20**, 4337–4345.

28. S. Choi, S. Lee, J. Park, W. T. Nichols and D. Shin, *Appl. Surf. Sci.*, 2018, **444**, 10–14.

29. X. Li, J. Liang, N. Chen, J. Luo, K. R. Adair, C. Wang, M. N. Banis, T. K. Sham, L. Zhang, S. Zhao, S. Lu, H. Huang, R. Li and X. Sun, *Angew. Chem., Int. Ed.*, 2019, **58**, 16427–16432.

30. J. Woo, Y. Song, H. Kwak, S. Jun, B. Jang, J. Park, K. Kim, C. Park, C. Lee, K.-. Park, Ho, H.-w. Lee and Y. S. Jung, *Adv. Energy Mater.*, 2023, **13**, 2203292.

31. Y. Choi, K. Park, D. Kim, D. Oh, H. Kwak, Y.-G. Lee and Y. Jung, *ChemSusChem.*, 2017, **10**, 2605–2611.

32. K. Park, D. Oh, Y. Choi, Y. Nam, L. Han, J.-y. Kim, H. Xin, F. Lin, S. Oh and Y. Jung, *Adv. Mater.*, 2016, **28**, 1874–1883.

33. L. Dhivya, K. Karthik, S. Ramakumar and R. Murugan, *RSC Adv.*, 2015, **5**, 96042–96051.

34. A. A. Raskovalov, E. A. Il'Ina and B. D. Antonov, *J. Power Sources*, 2013, **238**, 48–52.

35. M. Zhang, K. Takahashi, N. Imanishi, Y. Takeda, O. Yamamoto, B. Chi, J. Pu and J. Li, *J. Electrochem. Soc.*, 2012, **159**, A1114.

36. F. Mizuno, A. Hayashi, K. Tadanaga and M. Tatsumisago, *Solid State Ion.*, 2006, **177**, 2721–2725.

37. Y. Seino, T. Ota, K. Takada, A. Hayashi and M. Tatsumisago, *Energy Environ. Sci.*, 2014, **7**, 627–631.

38. K. Minami, A. Hayashi and M. Tatsumisago, *J. Ceram. Soc. Jpn.*, 2010, **118**, 305–308.

39. S. Boulineau, M. Courty, J. M. Tarascon and V. Viallet, *Solid State Ion.*, 2012, **221**, 1–5.

40. N. Kamaya, K. Homma, Y. Yamakawa, M. Hirayama, R. Kanno, M. Yonemura, T. Kamiyama, Y.

Kato, S. Hama, K. Kawamoto and A. Mitsui, *Nat. Mater.*, 2011, **10**, 682-686.

41. X. Li, J. Liang, J. Luo, M. N. Banis, C. Wang, W. Li, S. Deng, C. Yu, F. Zhao and Y. Hu, *Energy Environ. Sci.*, 2019, **12**, 2665–2671.

42. K. Homma, M. Yonemura, T. Kobayashi, M. Nagao, M. Hirayama and R. Kanno, *Solid State Ion.*, 2011, **182**, 53−58.

43. J. K. Feng, L. Lu and M. O. Lai, *J. Alloys Compd.*, 2010, **501**, 255−258.

44. J. W. Heo, A. Banerjee, K. Park, Y. Jung and S. Hong, *Adv. Energy Mater.*, 2018, **8**, 1702716.

45. T. Kim, K. Park, Y. Choi, J. Lee and Y. Jung, *J. Mater. Chem. A*, 2018, **6**, 840–844.

46. T. Asano, A. Sakai, S. Ouchi, M. Sakaida, A. Miyazaki and S. Hasegawa, *Adv. Mater.*, 2018, **30**, 1803075.